

# A Fourth Neutrino and its Consequences on CP Asymmetries

D. Delepine,<sup>1,\*</sup> C. Lujan-Peschard,<sup>1,†</sup> and M. Napsuciale<sup>1,‡</sup>

<sup>1</sup>*Departamento de Física, División de Ciencias e Ingeniería,  
Universidad de Guanajuato-Campus León, Lomas del Bosque 103,  
Fraccionamiento Lomas del Campestre, 37150, León, Guanajuato, México.*

A general analysis of the consequences of including a fourth neutrino in the standard model matter content, on CP violating observables at neutrino oscillation experiments, is presented. Neutrino oscillations in vacuum and with matter effects are studied. For the former we update and generalize previous studies on CP asymmetries with an additional active neutrino using an updated fit of the PMNS mixing matrix. We study the values of the new CP violating phases which maximize the different CP asymmetries in T2K and MINOS-like setups aiming to elucidate if the new phases yield measurable effects in the most favorable case. We show that due to a combined effect of kinematics and unitarity it is possible to obtain an observable asymmetry in the survival channels without violating CPT. For the MINOS-like setup, we find maximum asymmetries in vacuum of the order of 2% and 4% for the  $\nu_\mu \rightarrow \nu_e$  and  $\nu_e \rightarrow \nu_\tau$  channels respectively. For the T2K-like setup we obtain maximum asymmetries of the order of 6% in the survival  $\nu_\mu \rightarrow \nu_\mu$  channel. Tree level matter effects enhance the former reaching asymmetries of the order of 10% for the  $\nu_\mu \rightarrow \nu_e$  and  $\nu_e \rightarrow \nu_\tau$  channels, while the  $\nu_\mu \rightarrow \nu_\mu$  survival channel changes slightly depending on the mass hierarchy. Box diagrams with the fourth mass eigenstate as a virtual particle were also considered, the corrections to the scattering amplitude being negligible.

PACS numbers: 14.60.Pq; Neutrino oscillations. 14.60.St; Neutrinos in nonstandard model

## I. INTRODUCTION

The standard model yields a precise description of the fundamental interactions. Nevertheless, in the neutrino sector there are still observed phenomena whose proper description requires the introduction of new elements. Indeed, on one side the tiny neutrino squared mass differences suggests very small neutrino masses whose explanation requires the introduction of new heavy fields; on the other side, we have not been able to explain the short-baseline anomalies such as the LSND signal [1], the Mini-BooNE excesses [2], and the reactor anomaly [3].

The standard picture includes 3 active neutrinos whose mixing is described by the Pontecorvo-Maki-Nakagawa-Sakata (PMNS) matrix. The mixing angles and mass differences have been measured in different experiments which are designed to maximize a desired effect depending on the source, baseline and energy. The last parameter to be measured

was the mixing angle  $\theta_{13}$  [4, 5], that was for a long time assumed to be zero.

In this work we explore the consequences on CP asymmetries in neutrino oscillations due to the very existence of an additional heavy neutrino. As measured on LEP, the invisible width of the  $Z$  boson imposes that an additional active neutrino must be heavier than  $m_Z/2$ , while LEP2 excluded a heavy charged lepton, that would be the doublet partner of the neutrino considered, up to 100 GeV [6]. The most attractive scheme would be to consider a fourth sequential chiral generation, and indeed, there are several motivations to consider this as a first attempt to modify the Standard Model (SM). These have already been summarized in [7] and include: new CP Violation (CPV) source for the baryon asymmetry of the universe problem [8–11], new perspectives in the Higgs naturalness problem or in the fermion mass hierarchy problem [12–16]. However, the recent LHC (ATLAS and CMS) results put strong limits on the fourth generation Standard Model (SM4) since they have excluded at 95% a fourth generation down ( $b'$ ) and up quark ( $t'$ ) with masses smaller than  $m_{b'} < 611$  GeV [17–19] and  $m_{t'} < 557$  GeV [20–23]. Since these quarks cou-

\* delepine@fisica.ugto.mx

† carolup@fisica.ugto.mx

‡ mauro@fisica.ugto.mx

ple to the Higgs boson with a strength proportional to its mass, they do not decouple from the production of the Higgs boson. The existence of these extra fermions, regardless of their mass, would imply a Higgs boson  $M_H > 600$  GeV. Also precision electroweak observables constrain the difference of fourth generation quark and lepton masses [24–26].

In this paper though, we will make a discussion of the neutrino sector considering a fourth active neutrino regardless of the model in which it is embedded. Our goal is to test if the two extra CP violating phases that appear in the  $4 \times 4$  PMNS matrix can yield a sizable asymmetry in neutrino oscillations, hence we scan the whole parameter space for these phases obtaining those values that yields the maximum CP asymmetry in the different channels. For clarity and simplicity, we will start with the results obtained for neutrinos propagating in vacuum. We point how the somewhat surprising result of having a measurable asymmetry in the survival channel  $\nu_\mu \rightarrow \nu_\mu$  is obtained due to unitarity and kinematical constraints. Then we will proceed in an analogous analysis to the case of neutrinos propagating through matter for distances and energies that are comparable to current experiments. Finally, we will calculate the order of the corrections that could be induced in the scattering amplitude due to virtual effects of the heavy neutrino and its mixing with the light ones.

Our paper is organized as follows: in the next section we discuss neutrino oscillations in vacuum, the kinematics of the heavy neutrino and its impact on neutrino CP asymmetries. In section III we calculate the same observables in matter. In Section IV we calculate the box diagrams contributing at the next order in perturbation theory. Our conclusions are given in Section V and we give some details of the calculations in an appendix.

## II. NEUTRINOS IN VACUUM

The neutrino of flavour  $\alpha$ ,  $\nu_\alpha$ , is by definition the one that is produced in the weak interactions with its charged lepton partner  $W^+ \rightarrow l_\alpha^+ + \nu_\alpha$ , where  $\alpha = e, \mu$  or  $\tau$ . These are the interaction eigenstates which are related to the propagating states  $\nu_i$ ,  $i =$

1, 2, 3 through the PMNS matrix  $U_{\alpha i}$  as

$$|\nu_\alpha\rangle = \sum_i U_{\alpha i} |\nu_i\rangle. \quad (1)$$

The lagrangian for charged weak currents is given in terms of the propagating neutrino state as

$$\mathcal{L}_{cc} = -\frac{g}{\sqrt{2}} \sum_{\alpha,i} \bar{l}_{L\alpha} \gamma_\mu U_{\alpha i} \nu_{Li} W_+^\mu + h.c., \quad (2)$$

Several considerations are made in order to describe a neutrino state at a distance  $L$  from the production point and at a selected neutrino energy  $E$ . First, it is assumed that the neutrino mass eigenstate propagates as a plane wave, then we take the  $z$ -axis along the neutrino direction and consider that the propagating states are ultra-relativistic, i.e.,  $E_i \gg m_i$ . Under these assumptions one can easily find the neutrino state after a time  $t$  during which it travels a distance  $z$  [27–29]

$$|\nu_\alpha(t)\rangle = U_{\alpha 1} e^{-i\phi_1} |\nu_1\rangle + U_{\alpha 2} e^{-i\phi_2} |\nu_2\rangle + U_{\alpha 3} e^{-i\phi_3} |\nu_3\rangle, \quad (3)$$

where  $\frac{m_i^2}{2E_i} z \equiv \phi_i$ . The probability for oscillation of initial flavour  $\alpha$  to final flavour  $\beta$  is given by  $|\langle \nu_\beta | \nu_\alpha(t) \rangle|^2$  and a straightforward calculation yields

$$\begin{aligned} P_{\alpha\beta} = & 2\mathcal{R}(U_{\alpha 1} U_{\beta 1}^* U_{\alpha 2}^* U_{\beta 2}) [e^{-i(\phi_1 - \phi_2)} - 1] \\ & + 2\mathcal{R}(U_{\alpha 1} U_{\beta 1}^* U_{\alpha 3}^* U_{\beta 3}) [e^{-i(\phi_1 - \phi_3)} - 1] \\ & + 2\mathcal{R}(U_{\alpha 2} U_{\beta 2}^* U_{\alpha 3}^* U_{\beta 3}) [e^{-i(\phi_2 - \phi_3)} - 1] \end{aligned} \quad (4)$$

where the relation  $|a + b + c|^2 = |a|^2 + |b|^2 + |c|^2 + 2\mathcal{R}(ab^* + ac^* + bc^*)$  and the unitarity of the PMNS matrix are used. Equation (4) can also be written in the compact form

$$\begin{aligned} P_{\alpha\beta} = & -4 \sum_{i < j} \mathcal{R}(U_{\alpha i} U_{\beta i}^* U_{\alpha j}^* U_{\beta j}) \sin^2 \left( \frac{\phi_j - \phi_i}{2} \right) \\ & - 2 \sum_{i < j} \mathcal{I}(U_{\alpha i} U_{\beta i}^* U_{\alpha j}^* U_{\beta j}) \sin(\phi_j - \phi_i). \end{aligned} \quad (5)$$

It is clear that the second term in Eq. (5) in general will yield a difference in  $P_{\alpha\beta}$  with respect to  $P_{\bar{\alpha}\bar{\beta}}$  and this effect is driven by the phases in the PMNS matrix.

### A. The PMNS<sub>4×4</sub> Matrix and the Input Parameters.

A unitary  $n_g \times n_g$  matrix is parametrized by  $n_g^2$  parameters, out of which  $2n_g - 1$  phases may be reabsorbed by rephasing the fields. On the other hand, an orthogonal matrix of the same dimension can be parametrized by  $n_g(n_g - 1)/2$  angles. So a unitary complex  $n \times n$  matrix will have  $\frac{1}{2}(n_g - 1)(n_g - 2)$  physical phases. For  $n_g = 4$  we have 6 rotation angles and 3 phases. The PMNS <sub>$n_g \times n_g$</sub>  matrix can be written using the parametrization proposed in [30, 31] as

$$U = R_{n_g-1, n_g} \tilde{R}_{n_g-2, n_g} \dots \tilde{R}_{1, n_g} \dots R_{k-1, k} \dots R_{23} \tilde{R}_{13} R_{12}, \quad (6)$$

where  $\tilde{R}_{ij}$  is a complex rotation matrix on the  $ij$  axis and  $R_{ij}$  is the rotation without the phase. In the case  $n_g = 4$

$$U = (w_{34}(\theta_{34}) \times w_{24}(\theta_{24}, \varphi_3) \times w_{14}(\theta_{14}, \varphi_2)) \cdot (w_{23}(\theta_{23}) \times w_{13}(\theta_{13}, \delta) \times w_{12}(\theta_{12})). \quad (7)$$

In the calculation of the CP asymmetries below we will use for the conventional angles and differences of squared masses the best fit points from [32]. Although there are more recent reports on the value of  $\theta_{13}$ , i.e. [4, 5, 33, 34], the measured values are consistent with those of [32] and we prefer to work with the set of parameters that were used in the fit in a single analysis that considers the three neutrinos. As can be seen from Fig. 6 in [32], in this long baseline neutrino experiment is not possible to disentangle the values of  $\delta$  and  $\theta_{13}$ , so we decided to keep the best fit point which yields  $\delta = 0$ .

The upper bounds on the additional parameters due to the existence of a fourth neutrino are obtained from deviations of the unitarity of the PMNS matrix. In this concern, considering electroweak decays, such as, W decay, invisible Z decay, test of universality and rare decays, which lead to upper bounds for the product  $(NN^\dagger)_{\alpha\beta} = (HV(HV)^\dagger)_{\alpha\beta}$ , where  $N$  is the non-unitary PMNS matrix composed of a hermitian ( $H$ ) and a unitary ( $V$ ) matrix, robust bounds for deviations of unitarity of the PMNS matrix were obtained in [35] which updates previous studies in [36, 37]. We use the results reported in [35] to extract the upper

Parameter	Value	Reference
$\theta_{12}$	$34.4^\circ$	[32]
$\theta_{13}^*$	$9.68^\circ$	[32]
$\theta_{23}$	$45^\circ$	[32]
$\delta^*$	$0^\circ$	[32]
$\Delta m_{21}^2$	$7.6 \times 10^{-5} \text{ eV}^2$	[32]
$\Delta m_{32}^2$	$2.4 \times 10^{-3} \text{ eV}^2$	[32]
$\theta_{14}$	$< 3.62^\circ$	
$\theta_{24}$	$< 2.29^\circ$	
$\theta_{34}$	$< 4.21^\circ$	
$m_4$	$\approx 100 \text{ GeV}$	

TABLE I. Input parameters assuming the Normal Hierarchy (NH). Two variables marked with \* are correlated and we take their best fit values.

bounds on the the additional angles due to the existence of a fourth neutrino. Relating these bounds to the 3 new angles, we obtained:  $\theta_{14} < 3.62^\circ$ ,  $\theta_{24} < 2.29^\circ$  and  $\theta_{34} < 4.21^\circ$ . Notice that we have left the extra CP phases,  $\varphi_2$  and  $\varphi_3$ , as free parameters and that from now on we will have a complex PMNS matrix. We use the input parameters shown in Table I, with  $\Delta m_{ij}^2 \equiv m_i^2 - m_j^2$ . For the Normal Hierarchy (NH)  $\Delta m_{31}^2 = \Delta m_{32}^2 + \Delta m_{21}^2$ , whereas for the inverted hierarchy (IH) we used instead  $\Delta m_{31}^2 = -2.4 \times 10^{-3} \text{ eV}^2$  and  $\theta_{13} = 10.99^\circ$ .

### B. Neutrino Oscillations with an Extra Heavy Neutrino

If a fourth neutrino exists, it is necessarily heavy with a mass well above the present energies of neutrino beams, thus the oscillation of a light neutrino ( $\nu_e, \nu_\mu, \nu_\tau$ ) into a heavy neutrino denoted hereafter as  $\nu_E$  is kinematically forbidden. In spite of this, the very existence of such neutrino implies the appearance of new phases in the PMNS matrix which manifest in observable CP violation effects yielding asymmetries in the probabilities for neutrino oscillations with respect to those of the antineutrinos. Furthermore, as we will show below, the interference with light neutrinos produces interesting effects and even in the diagonal channels (surviving probabilities) there can be an observable asymmetry due to the combined effects of the new phases,

unitarity and the kinematics of the oscillations.

We consider first the propagation of neutrinos. In general, the proper calculation of the neutrino state at a given time requires to solve the corresponding wave equation whose complete form is still unknown due to the lack of information on the nature of the mass term. However, as far as the neutrinos do not interact with other fields while traveling, Lorentz covariance allows to write the neutrino state as

$$\psi(t) = \psi(0)e^{-ip \cdot x} = \psi(0)e^{-i(Et - |\mathbf{p}|L)} \quad (8)$$

and the specific form of the state  $\psi(0)$  is not required beyond the fact that it coincides with the states produced in weak interactions. The weak eigenstates are linear combinations of the neutrino mass eigenstates which satisfy the eigenvalue equation  $H|\nu_a\rangle = E_a|\nu_a\rangle$ ,  $a = 1, 2, 3, 4$ , thus they have a component along the fourth neutrino

$$|\nu_\alpha\rangle = U_{\alpha 1}|\nu_1\rangle + U_{\alpha 2}|\nu_2\rangle + U_{\alpha 3}|\nu_3\rangle + U_{\alpha 4}|\nu_4\rangle \quad (9)$$

The fourth component is rapidly damped by the kinematics during the propagation. Indeed, in contrast to the light neutrinos, a heavy one propagates non-relativistically and we can estimate the size of this component at a time  $t$  by a simple quantum mechanical calculation. The kinematical suppression of this component during the propagations can be seen as an imaginary momentum according to

$$|\mathbf{p}| \equiv -i\omega, \quad \omega = \sqrt{m^2 - E^2}. \quad (10)$$

Performing a non-relativistic expansion it is straightforward to show that

$$-i(Et - |\mathbf{p}|L) = -mL \left[ 1 + \mathcal{O}\left(\frac{E}{m}\right) \right]. \quad (11)$$

We conclude that for the fourth heavy neutrino instead of a phase we have an exponential damping factor  $e^{-mL}$  which kills this component after a distance of order  $1/m$ . For instance, considering a 100 GeV mass eigenstate this component disappears after a distance of the order of  $10^{-3}$  fm. The propagation effects of a fourth heavy neutrino seem to be completely irrelevant. We remark however that due to the propagation of  $|\nu_i\rangle$  and the mixing of the

neutrinos, at a given time the state  $|\nu(t)\rangle$  contains a non-vanishing component of the heavy weak eigenstate  $|\nu_E\rangle$  and there is a non-vanishing probability for the oscillation to this state. Of course, at the present beam energies this oscillation is forbidden by the kinematics, but then the effects of this non-vanishing probability manifest via unitarity.

In order to explore the possible effects we now calculate the oscillation probabilities in the presence of a fourth neutrino. The generalization of Eq. (4) is straightforward

$$P_{\alpha\beta} = 2 \sum_{i < j} \mathcal{R}(U_{\alpha i} U_{\beta i}^* U_{\alpha j}^* U_{\beta j}) [e^{-i(\phi_i - \phi_j)} - 1] 2 + \sum_i 2 \mathcal{R}(U_{\alpha i} U_{\beta i}^* U_{\alpha 4}^* U_{\beta 4}) (e^{-i\phi_i} e^{-mL} - 1).$$

Neglecting the term containing the damping factor we get the generalization of Eq. (5) as

$$P_{\alpha\beta} = -4 \sum_{i < j} \mathcal{R}(U_{\alpha i} U_{\beta i}^* U_{\alpha j}^* U_{\beta j}) \sin^2 \left( \frac{\phi_j - \phi_i}{2} \right) - 2 \sum_{i < j} \mathcal{I}(U_{\alpha i} U_{\beta i}^* U_{\alpha j}^* U_{\beta j}) \sin(\phi_j - \phi_i) \quad (13) + 2 \sum_i \mathcal{R}(U_{\alpha i} U_{\beta i}^* U_{\alpha 4}^* U_{\beta 4}).$$

There are three major modifications due to the existence of a fourth neutrino: i) the new phases modify the second term in Eq. (13) yielding new sources for CP violation and CP asymmetries; ii) the appearance of the last term in this equation; and iii) the modification of unitarity relations. In the following we explore the consequences of these modifications for the asymmetries in neutrino oscillations.

### C. Symmetry Transformations and the Oscillation Probabilities

The symmetry transformations **T**, **CP** y **CPT** map the following neutrino oscillations amplitudes

$$\mathbf{T} : \nu_\alpha \rightarrow \nu_\beta \implies \nu_\beta \rightarrow \nu_\alpha \quad (14)$$

$$\mathbf{CP} : \nu_\alpha \rightarrow \nu_\beta \implies \bar{\nu}_\alpha \rightarrow \bar{\nu}_\beta \quad (15)$$

$$\mathbf{CPT} : \nu_\alpha \rightarrow \nu_\beta \implies \bar{\nu}_\beta \rightarrow \bar{\nu}_\alpha, \quad (16)$$

thus **CPT** symmetry requires

$$P_{\beta\alpha} = P_{\bar{\alpha}\bar{\beta}}. \quad (17)$$

On the other hand, exchanging  $\nu_\alpha \leftrightarrow \nu_\beta$  in Eq. (5), if the PMNS matrix is complex we get

$$P_{\alpha\beta} \neq P_{\beta\alpha}. \quad (18)$$

This means that the weak interactions are not invariant under the **CP** (or **T**) transformation. Combining the results in Eqs. (17,18), for a complex PMNS matrix we get

$$P_{\alpha\beta} \neq P_{\bar{\alpha}\bar{\beta}}, \quad (19)$$

and in general it is possible to test **CP** symmetry in weak interactions by considering asymmetries in neutrino oscillations.

Concerning the surviving probabilities, **CPT** symmetry requires

$$P_{\alpha\alpha} = P_{\bar{\alpha}\bar{\alpha}} \quad (20)$$

hence **CP** asymmetries should not show in the survival probabilities. However, the transitions to the heavy state are forbidden by kinematics and this manifests in observable oscillation asymmetries even in these channels. Indeed, probability conservation requires

$$P_{\alpha\alpha} = 1 - \sum_{\beta \neq \alpha} P_{\alpha\beta}, \quad (21)$$

where  $\beta = e, \mu, \tau, E$ . Similarly

$$P_{\bar{\alpha}\bar{\alpha}} = 1 - \sum_{\beta \neq \alpha} P_{\bar{\alpha}\bar{\beta}}, \quad (22)$$

Thus, using both unitarity and **CPT** symmetry we get

$$\sum_{\beta \neq \alpha} P_{\alpha\beta} = \sum_{\beta \neq \alpha} P_{\bar{\alpha}\bar{\beta}} \quad (23)$$

i.e., **CP** violation effects cancel in the sum over all the channels. However, in spite of being allowed by the dynamics, for present beam energies well below the heavy neutrino mass, the transition of a light neutrino into the heavy one is forbidden by the kinematics. On the other hand for a complex PMNS matrix from Eq. (13) we get

$$P_{\alpha E} \neq P_{\bar{\alpha}\bar{E}} \quad (24)$$

then the combined effect of kinematics, unitarity and **CP** violation is a measurable asymmetry in the survival channels even if **CPT** is a good symmetry, e.g. for the muon neutrinos, due to the kinematically forbidden transition with probabilities  $P_{\alpha E}$  and  $P_{\bar{\alpha}\bar{E}}$ , in an experiment in general we will obtain

$$1 - P_{\mu e} - P_{\mu\tau} \neq 1 - P_{\bar{\mu}\bar{e}} - P_{\bar{\mu}\bar{\tau}}. \quad (25)$$

#### D. CP Asymmetries

In this section we study the size of the effects of a heavy neutrino in neutrino oscillations asymmetries as a function of the involved parameters. The sizeable effects of a heavy neutrino in **CP** asymmetries were shown in [38] in the case where the extra phases are fixed to  $\pi/2$ . This part of our calculation updates the input and generalizes results in [38] to scan the whole parameter space for the new phases and to keep the PMNS matrix elements corresponding to the fourth neutrino independent and within the maximal values allowed by unitarity.

We start by fixing the beam energy and baseline to the MINOS (M) and T2K (T) type setup, leaving the new phases as free parameters and finding the values maximizing the effects. For  $E$  we use the mean beam energy in both cases. The specific values used in the calculation are given in Table II. For each channel we obtain the values of the new phases maximizing the **CP** asymmetry

$$A_{CP} = \frac{P_-}{P_+}, \quad \text{where } P_{\pm} = P_{\alpha\beta} \pm P_{\bar{\alpha}\bar{\beta}}. \quad (26)$$

The explicit expressions for the asymmetry in terms of the angles and phases characterizing the PMNS matrix are lengthy, so we only give in the appendix a simplified expression in the channel  $\nu_\mu \rightarrow \nu_e$ , where the effects of the new phases are visible. We will not consider at all times the last term in Eq. (13) since the modifications to the asymmetries due to it are negligible.

Our results for the **CP** asymmetry in the  $\nu_\mu \rightarrow \nu_e$  oscillation channel are shown in Fig. 1 and those of the  $\nu_\mu \rightarrow \nu_\mu$  survival channel are depicted in Fig. 2.



Experiment	$L$ [km]	$\langle E_\nu \rangle$ [GeV]
T2K (T)	295	0.6
MINOS (M)	735	3.0

TABLE II. Values used in the calculation of CP asymmetries

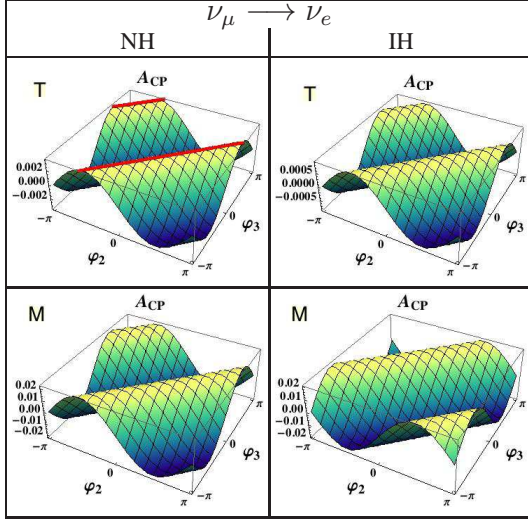


FIG. 1. CP asymmetry in the  $\nu_\mu \rightarrow \nu_e$  channel for the T and M parameters, considering the normal (NH) and inverted hierarchies (IH).

In these plots we can see the maximum values reached by the corresponding CP asymmetry and its dependence on the new phases. For the  $\nu_\mu \rightarrow \nu_e$  channel there are regions in the parameter space yielding similar values for the maximum CP asymmetries as shown with a line in the upper left plot in Figure 1. Also, it is remarkable that the survival  $\nu_\mu \rightarrow \nu_\mu$  channel has the biggest asymmetry when evaluated for the T parameters. Comparing between the two hierarchies we find a maximum asymmetry 4 times bigger for the normal hierarchy compared with the inverted hierarchy in the  $\nu_\mu \rightarrow \nu_e$  channel and for the T parameters. For the remaining channels we have a small variation for both, T and M parameters. We have studied all the channels finding the maximum asymmetries and the corresponding phases for each channel given in Table III. We find that the most favoured channels are the  $\nu_\mu \rightarrow \nu_\mu$

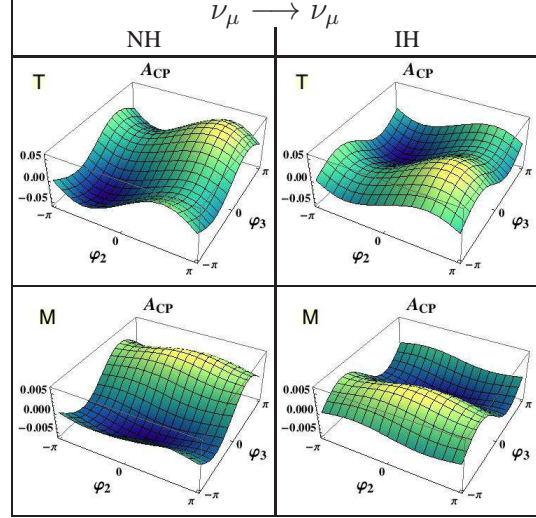


FIG. 2. CP asymmetry in the survival channel  $\nu_\mu \rightarrow \nu_\mu$  for the T and M parameters, considering normal (NH) and inverted (IH) hierarchies.

survival channel for T-like setup and the  $\nu_e \rightarrow \nu_\tau$  channel for the M-like setup which yield maximum asymmetries of the order of 5%.

T-like				
	$\nu_\mu \rightarrow \nu_e$	$\nu_\mu \rightarrow \nu_\tau$	$\nu_e \rightarrow \nu_\tau$	$\nu_\mu \rightarrow \nu_\mu$
NH $\varphi_2$	$-93.66^\circ$	$-108.77^\circ$	$92.81^\circ$	$100.30^\circ$
NH $\varphi_3$	$175.21^\circ$	$-70.07^\circ$	$-88.26^\circ$	$101.39^\circ$
NH $A_{CP}$	0.3%	0.1%	0.5%	5.9%
IH $\varphi_2$	$-35.09^\circ$	$-71.42^\circ$	$92.19^\circ$	$102.71^\circ$
IH $\varphi_3$	$-126.11^\circ$	$70.35^\circ$	$-88.06^\circ$	$75.80^\circ$
IH $A_{CP}$	0.1%	0.1%	0.7%	5.7%

M-like				
	$\nu_\mu \rightarrow \nu_e$	$\nu_\mu \rightarrow \nu_\tau$	$\nu_e \rightarrow \nu_\tau$	$\nu_\mu \rightarrow \nu_\mu$
NH $\varphi_2$	$-35.08^\circ$	$-110.42^\circ$	$-92.30^\circ$	$7.85^\circ$
NH $\varphi_3$	$-126.09^\circ$	$-89.35^\circ$	$-81.77^\circ$	$91.52^\circ$
NH $A_{CP}$	2.2%	0.7%	4.3%	0.6%
IH $\varphi_2$	$79.59^\circ$	$-65.38^\circ$	$91.80^\circ$	$8.68^\circ$
IH $\varphi_3$	$170.75^\circ$	$89.49^\circ$	$-79.97^\circ$	$-88.44^\circ$
IH $A_{CP}$	2.0%	0.7%	3.7%	0.6%

TABLE III. Values of the CP asymmetry and phases  $\varphi_2$  and  $\varphi_3$  that maximize it in vacuum.

For given values of the new phases we get very

different results for these setups and this lead us to study the asymmetries as a function of the baseline and of the neutrino beam energy. We are interested in the maximum asymmetry provided by the new phases, thus for a given value of  $E$  and  $L$  we scan the phases parameter space keeping those yielding the maximum asymmetry.

Our results for the maximum asymmetry as a function of  $L$  and  $E$  and floating phases  $\varphi_2$ ,  $\varphi_3$  are given in Figs. 3 and 4 respectively where we consider normal hierarchy.

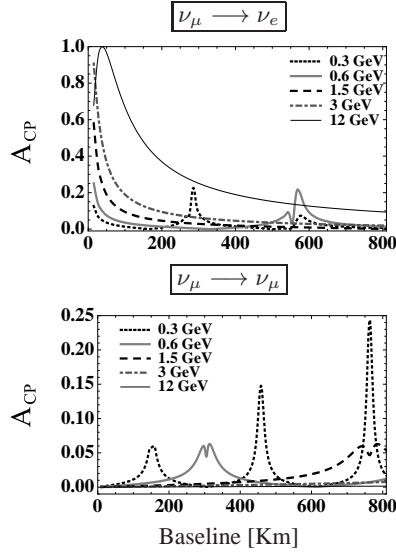


FIG. 3. Maximum CP asymmetry in the  $\nu_\mu \rightarrow \nu_e$  and  $\nu_\mu \rightarrow \nu_\mu$  channels as a function of the baseline considering NH. The curves correspond to selected beam energies from 0.3 GeV to 12 GeV.

In order to visualize the way the asymmetry behaves as a function of the baseline once the phases are fixed, we consider the T-like beam energy and evaluate in the phases corresponding to the maximum for the T setup. Our results for the  $\nu_\mu \rightarrow \nu_\mu$  channel with normal hierarchy are given in Fig. 5 where a variation of the order of 6% can be seen when varying the baseline.

From these plots we conclude that high energy neutrinos may give a big asymmetry for shorter baseline experiments in the appearance channels  $\nu_\mu \rightarrow \nu_e$ ,  $\nu_\mu \rightarrow \nu_\tau$  and  $\nu_e \rightarrow \nu_\tau$ . CP asymmetries

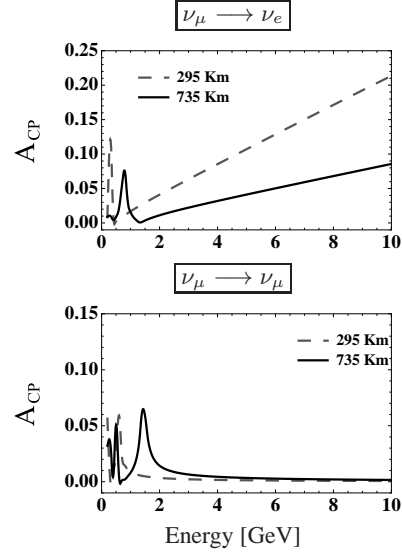


FIG. 4. Maximum CP asymmetry as a function of the neutrino's energy for a baseline of 295 Km and 735 Km considering the NH.

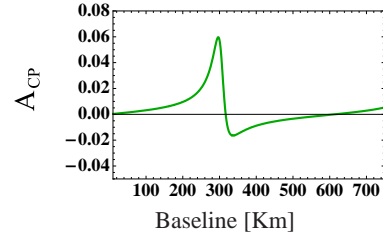


FIG. 5. CP Asymmetry for fixed  $\varphi_2$  and  $\varphi_3$  using the T energy of 0.6 GeV as a function of the baseline with the NH.

can be substantial for low energy neutrinos only for specific values of the baselines. We studied these observables using the inverted hierarchy obtaining similar results. It is interesting that sizeable asymmetries in the survival channel  $\nu_\mu \rightarrow \nu_\mu$ , can be obtained for low energy neutrinos, for example with a baseline between 700 and 800 km and  $E_\nu$  around 0.3 GeV, while there is almost no CP asymmetry when considering higher energy neutrinos.

### III. NEUTRINOS THROUGH MATTER

As originally pointed out in [39–41], there might be non negligible effects on neutrino oscillations due to the interactions with matter in which the neutrinos propagate. The interaction between neutrinos and matter components: protons, neutrons and electrons, is feeble but a considerable effect on the oscillation amplitude can be obtained by coherent forward scattering of neutrinos from many particles in the material medium.

At tree level, the neutral current (Z exchange in Fig. 6(a)) yields an identical contribution for all neutrino flavours and it only produces a shift in the energy eigenvalue  $E_i$ . This shift does not affect the oscillation probabilities, since it appears as an overall phase factor in the amplitude. The charged current breaks this picture since matter contains only electrons and at tree level the only process contributing is  $\nu_e e$  elastic scattering via the  $u$ -channel  $W$  exchange diagram shown in Figure 6b. At the present beam energies well below the  $W$  mass this diagram yields the following effective interaction

$$\begin{aligned} H_{eff} &= \frac{G_F}{\sqrt{2}} \bar{e} \gamma^\mu (1 - \gamma_5) \nu \bar{\nu} \gamma_\mu (1 - \gamma_5) e \quad (27) \\ &= \frac{G_F}{\sqrt{2}} \bar{e} \gamma^\mu (1 - \gamma_5) e \bar{\nu} \gamma_\mu (1 - \gamma_5) \nu \end{aligned}$$

where a Fierz transformation has been performed to obtain the result on the second line. With  $N_e \approx 1.5 N_A / \text{cm}^3$ , considering a constant density  $\rho \approx 3 \text{ g/cm}^3$ , the final correction to the energy is  $\sqrt{2} G_F N_e$ .

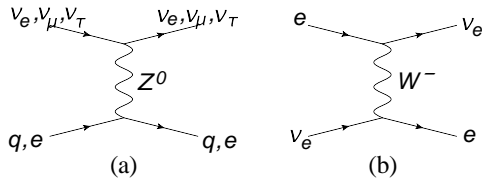


FIG. 6. Tree level diagrams for neutrino interactions with particles in matter.

Neutrino propagation in matter requires to take into account these interactions and the time evolution of an arbitrary state vector  $|\nu(t)\rangle =$

$\sum_i f_i(t) |\nu_i\rangle$  that will be driven by the equation [39–41]

$$\begin{aligned} i \frac{df_j(t)}{dt} &= \frac{m_j^2}{2E} f_j(t) + \sum_\alpha \sqrt{2} G_F N_e U_{ej}^* U_{ek} f_k(t) \\ &\equiv H_{jk} f_k(t). \end{aligned} \quad (28)$$

In [40] an iterative solution was found. The leading order for  $f_j^{(i)}$  ( $i = 1, \dots, n$ ) are

$$f_j^{(i)}(t=0) = \delta_{ij}. \quad (29)$$

Then, assembling the row vectors into a  $n \times n$  matrix  $X$  that satisfies the equation

$$i \frac{dX}{dt} = XH, \quad (30)$$

with the boundary condition  $X(t=0) = 1$  an analytical solution for (30) is possible for a constant electron density  $N_e$ . This approximation is valid if we restrict to  $L < 750 \text{ km}$ .

We use the results in [40] and scan the parameter space for the new phases to obtain the maximum CP asymmetry in a T-like experiment. Our results are shown in Figs. 7, 8. The asymmetries in general are bigger for the channels that involve  $\nu_e$  as expected. While the results for the other channels show the same dependence on the neutrino energy compared to the vacuum case, in this channel the low energy neutrinos show an enhancement providing a considerable asymmetry. In the survival channel a variation that depends on the hierarchy is found for the low energy neutrinos with respect to the vacuum result.

### IV. BOX DIAGRAMS WITH VIRTUAL HEAVY NEUTRINO

Although box diagrams are suppressed with respect to the tree level contributions, enhancements of the matter effects can occur when we consider a heavy neutrino [42]. Fig. 9a shows a box diagram that has already been calculated in [42], along with other one-loop diagrams representing the whole  $\mathcal{O}(\alpha m_\tau^2 / M_W^2)$  electroweak radiative corrections to coherent forward neutrino scattering. Here we do not consider the whole set of diagrams, since



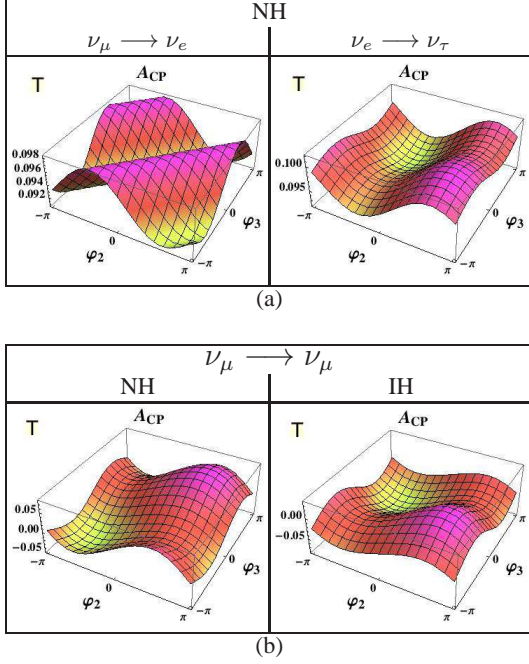


FIG. 7. CP asymmetry in the (a)  $\nu_\mu \rightarrow \nu_e$  and the  $\nu_e \rightarrow \nu_\tau$  channels with NH (b)  $\nu_\mu \rightarrow \nu_\mu$  channel for the normal (NH) and inverted (IH) hierarchy for the T-like experiment parameters considering matter effects.

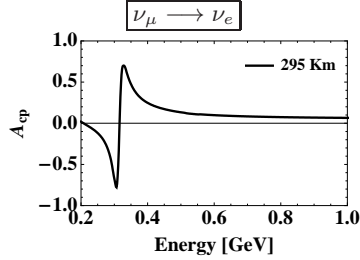


FIG. 8. CP asymmetry in the  $\nu_\mu \rightarrow \nu_e$  channel with low energy neutrinos considering matter effects.

we are interested only in diagrams with a virtual heavy neutrino, therefore we focus on the box diagrams. We also consider as a possibility the diagrams shown on Figures 9b and 9c, where we can have neutrino flavour changing weak interactions since the virtual propagating neutrino is a mass

eigenstate, thus we have the possibility of having these processes with different neutrino flavours as outer legs.

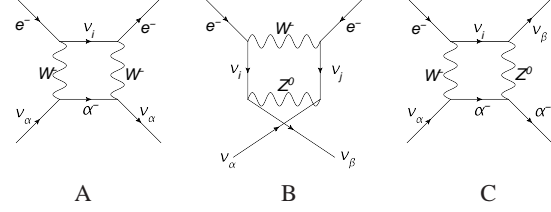


FIG. 9. Box diagrams with a virtual heavy neutrino for neutrino propagation through matter.

The evaluations were performed using dimensional regularization and the Feynman gauge ( $\xi = 1$ ). We considered the zero external momentum approximation, which is a good approximation for neutrino energies below 20 GeV.

The diagrams with the corresponding Goldstone bosons turn out to be negligible, since they depend on powers of neutrino masses of the first three generations. For simplicity we stick to the normal hierarchy with the mass eigenstate  $\nu_4$  being the most massive and used the lower bound on  $m_{\nu_4} = 100$  GeV. We would expect this one to be mostly  $\nu_E$  with little components of the three standard flavours, since the mixing angles are very small. We used for  $\varphi_2$  and  $\varphi_3$ , that appear in the relevant PMNS matrix elements, the values that maximize the CP asymmetry of the T parameters for the NH in each of the channels. It is only in the case of the flavour changing process that the extra CP violating phases enter into the expressions. In summary our results are the following:

A) For this diagram the most relevant contribution to the amplitude comes from the light neutrinos  $\nu_i$ ,  $i = 1, 2, 3$  as intermediate states. For an incoming electronic neutrino the absolute value of the amplitude from this diagram is of order  $2 \times 10^{-7}$ . The absolute value for the tree level amplitudes is  $0.4 \times 10^{-4}$ , hence the ratio to the tree level diagram is of order  $5 \times 10^{-3}$ . Amplitudes with incoming  $\nu_\mu$ ,  $\nu_\tau$  are even smaller.

B) This diagram allows for neutrino flavour changing processes. For an incoming electronic neutrino and flavour conserving diagrams the ratio

to the tree level diagram is of the order of  $8 \times 10^{-4}$  while for flavour violating diagrams the absolute value of the amplitude is of the order of  $10^{-10}$ . Considering an incoming muonic neutrino with a final neutrino either muonic or taonic the order is even smaller, namely  $\sim 10^{-12}$ .

C) This diagram admits also change in neutrino flavour. For an incoming electronic neutrino the ratio to the tree level process in the  $ee$  is  $\sim 2 \times 10^{-3}$ , amplitudes for other flavour conserving processes and amplitudes for flavour violating processes are at least two orders of magnitude smaller.

Summarizing this section we conclude that the amplitudes of the three box diagrams are at least 3 orders of magnitude smaller than the tree level amplitude and numerically have no impact in the asymmetries in neutrino oscillations.

## V. CONCLUSIONS

The very existence of a fourth neutrino modifies the conventional PMNS mixing matrix introducing three new angles and two new phases yielding new possible sources for CP violation. Since the mixing with light neutrinos is small it is desirable to have an estimate of the size of the CP violation effects in current neutrino experiment.

In this work we studied the maximum values that CP asymmetries in neutrino oscillations can reach when a fourth neutrino is considered, both in vacuum and in the presence of matter. We show that another consequence of the existence of a fourth neutrino is that it is possible to observe asymmetries in the surviving channels even if CPT is conserved, due to a combined effect of unitarity, kinematics and CP violation.

In the numerics we set the value of the phase appearing in the case of three neutrinos to  $\delta = 0$ , so that the imaginary part of the PMNS matrix is due entirely to the existence of the fourth neutrino. Using the upper bound values for the three extra mixing angles as obtained from the deviations from unitarity studies [35], we got  $\theta_{14} < 3.62^\circ$ ,  $\theta_{24} < 2.29^\circ$  and  $\theta_{34} < 4.21^\circ$ . We study the maximum asymmetries that can be reached in neutrino oscillation as functions of the neutrino energy, the distance to the detector and the two new phases, scanning the

whole parameter space for the latter.

Our analysis shows that, under the above assumptions, in vacuum, the maximum asymmetries that can be reached in a T2K-like setup ( $L = 295$  km,  $E_\nu = 0.6$  GeV) are of the order of 6% and appear in the survival  $\nu_\mu \rightarrow \nu_\mu$  channel. Asymmetries in other channels are at least one order of magnitude smaller. As for the MINOS-like setup ( $L = 735$  km,  $E_\nu = 3$  GeV), the maximum asymmetries can be reached in the  $\nu_e \rightarrow \nu_\tau$  and  $\nu_\mu \rightarrow \nu_e$  channel and are of the order of 4% and 2% respectively. Importantly, for the same baseline but a different energy within the reach of MINOS, namely  $E_\nu = 1.4$  GeV, we get a maximum asymmetry of the order of 6% in the surviving  $\nu_\mu \rightarrow \nu_\mu$  channel.

Effects of matter enhance the maximal asymmetry in the channels involving electronic neutrinos as expected. For the T2K-like setup the maximum asymmetry in the  $\nu_\mu \rightarrow \nu_e$  channel raises from 0.3% in vacuum to 9% in the presence of matter, while for  $\nu_e \rightarrow \nu_\tau$  it grows from 0.5% in vacuum to 10% in a material medium. In these channels results for the maximal asymmetries are similar with normal and inverted hierarchy. The interaction with matter has a small indirect effect in the survival  $\nu_\mu \rightarrow \nu_\mu$  channel via unitarity, whose sign depends on the hierarchy. It goes from the order of 6% in vacuum, independently of the hierarchy, to 8% in matter for normal hierarchy, while it decreases to 4% in the case of an inverted hierarchy.

The value of the asymmetry in the  $\nu_\mu \rightarrow \nu_e$  channel varies with the energy of the neutrino beam in general being larger at low energies. For the T2K baseline, as shown in Fig. (8) the maximum asymmetries can be of the order of 70% changing the sign when going from beam energies of  $E_\nu = 0.30$  GeV to  $E_\nu = 0.33$  GeV. Although not shown explicitly, for a fixed energy below 1 GeV we obtain similar peaks in the maximum asymmetries for definite values of  $L$ . For the T2K energy  $E_\nu = 0.6$  GeV the peaks appear around  $L = 550$  km.

We do not report the obtained asymmetries in matter in the case of MINOS-like because in this case the baseline is at the edge of the validity of the approximations used in the solution of the propagating equations and a deeper analysis beyond the scope of this work is necessary in this case.

The potential contributions to the  $\nu e$  scattering

amplitude due to the exchange of virtual heavy neutrinos in box diagrams were found to be negligible.

Finally we would like to remark that the possibility to have an asymmetry in the surviving channel  $\nu_\mu \rightarrow \nu_\mu$  is a consequence of the very existence of a fourth neutrino, thus it would be interesting to try an experimental search of this channel since the measurement of an asymmetry in this channel would be a direct proof of the existence of a fourth neutrino with important implications in particle physics and cosmology.

### ACKNOWLEDGMENTS

Work supported by CONACyT México under project 156618.

### Appendix A: CP Asymmetry for $\nu_\mu \rightarrow \nu_e$

In order to sketch the way to obtain the asymmetry we will consider the  $\nu_\mu \rightarrow \nu_e$  channel with some simplifying assumptions, namely that  $\sin^2 2\theta_{13} = 0$ , in contrast with the assumptions in the rest of this work. As a notation we will simplify  $s_{ij} = \sin \theta_{ij}$ ,  $c_{ij} = \cos \theta_{ij}$  and  $\Delta_{ij} = \Delta m_{ij}^2 L / (4E)$ . In this case the probability for particle and antiparticle oscillations are given by

$$P_{\mu e(\bar{\mu} \bar{e})} = s_{24}^2 s_{14}^2 c_{14}^2 (c_{12}^4 + s_{12}^4) + 2c_{24}^2 c_{14}^2 c_{23}^2 s_{12}^2 c_{12}^2 (1 - \cos \Delta_{21}) \quad (\text{A1})$$

$$+ 2s_{24}c_{24}s_{14}c_{14}^2 c_{23}s_{12}c_{12}^3 \cos(\varphi_2 - \varphi_3) - 2s_{24}c_{24}s_{14}c_{14}^2 c_{23}s_{12}^3 c_{12} \cos(\varphi_2 - \varphi_3)$$

$$+ 2s_{24}^2 s_{14}^2 c_{14}^2 s_{12}^2 c_{12}^2 \cos \Delta_{21} \pm 2s_{24}c_{24}s_{14}c_{14}^2 c_{23}s_{12}c_{12} \sin(\varphi_2 - \varphi_3) \sin 2\Delta_{21}$$

$$- 2s_{24}c_{24}s_{14}c_{14}^2 c_{23}s_{12}c_{12}^3 \cos(\varphi_2 - \varphi_3) \cos \Delta_{21} + 2s_{24}c_{24}s_{14}c_{14}^2 c_{23}s_{12}^3 c_{12} \cos(\varphi_2 - \varphi_3) \cos \Delta_{21}$$

where we neglect the last term in Eq. (13). The difference in the probabilities is given in this case as

$$P_- = 4s_{24}c_{24}s_{14}c_{14}^2 c_{23}s_{12}c_{12} \sin(\varphi_2 - \varphi_3) \sin \Delta_{21} \quad (\text{A2})$$

- 
- [1] A. Aguilar *et al.* [LSND Collaboration], Phys. Rev. D **64**, 112007 (2001) [arXiv:hep-ex/0104049]
  - [2] A. A. Aguilar-Arevalo *et al.* [MiniBooNE Collaboration], Phys. Rev. Lett. **105**, 181801 (2010) [arXiv:1007.1150 [hep-ex]].
  - [3] G. Mention *et al.* Phys. Rev. D **83**, 073006 (2011) [arXiv:1101.2755 [hep-ex]].
  - [4] J. K. Ahn *et al.* [RENO Collaboration], Phys. Rev. Lett. **108**, 191802 (2012) [arXiv:1204.0626 [hep-ex]].
  - [5] F. P. An *et al.* [Daya Bay Collaboration], Phys. Rev. Lett. **108**, 171803 (2012). [arXiv:1203.1669 [hep-ex]].
  - [6] K. Nakamura *et al.* [Particle Data Group], J. Phys. G **37**, 075021 (2010).
  - [7] B. Holdom, W. S. Hou, T. Hurth, M. L. Mangano, S. Sultansoy, G. Ünel. PMC Phys. A **3**, 4 (2009). [arXiv:0904.4698 [hep-ph]].
  - [8] W. -S. Hou, Chin. J. Phys. **47**, 134 (2009) [arXiv:0803.1234 [hep-ph]].
  - [9] G. W. S. Hou, Int. J. Mod. Phys. D **20**, 1521 (2011) [arXiv:1101.2161 [hep-ph]].
  - [10] R. Fok and G. D. Kribs, Phys. Rev. D **78**, 075023 (2008) [arXiv:0803.4207 [hep-ph]].
  - [11] S. W. Ham, S. K. Oh and D. Son, Phys. Rev. D **71**, 015001 (2005) [arXiv:hep-ph/0411012].

- [12] B. Holdom, Phys. Rev. Lett. **57**, 2496 (1986) [Erratum-ibid. **58**, 177 (1987)].
- [13] S. F. King, Phys. Lett. B **234**, 108 (1990).
- [14] C. T. Hill, M. A. Luty and E. A. Paschos, Phys. Rev. D **43**, 3011 (1991).
- [15] P. H. Frampton, P. Q. Hung and M. Sher, Phys. Rept. **330**, 263 (2000) [arXiv:hep-ph/9903387] and references within.
- [16] D. Delepine, M. Napsuciale and C. A. Vaquera-Araujo, Phys. Rev. D **84**, 033008 (2011) [arXiv:1003.3267 [hep-ph]].
- [17] S. Chatrchyan *et al.* [CMS Collaboration], JHEP **1205**, 123 (2012) [arXiv:1204.1088 [hep-ex]].
- [18] G. Aad *et al.* [ATLAS Collaboration], arXiv:1202.6540 [hep-ex].
- [19] T. Aaltonen *et al.* [CDF Collaboration], Phys. Rev. Lett. **106**, 141803 (2011) [arXiv:1101.5728 [hep-ex]].
- [20] S. Chatrchyan *et al.* [CMS Collaboration], arXiv:1203.5410 [hep-ex].
- [21] G. Aad *et al.* [ATLAS Collaboration], Phys. Rev. Lett. **108**, 261802 (2012) [arXiv:1202.3076 [hep-ex]].
- [22] G. Aad *et al.* [ATLAS Collaboration], arXiv:1202.3389 [hep-ex].
- [23] V. M. Abazov *et al.* [D0 Collaboration], arXiv:1104.4522 [hep-ex].
- [24] G. D. Kribs, T. Plehn, M. Spannowsky and T. M. P. Tait, Phys. Rev. D **76**, 075016 (2007) [arXiv:0706.3718 [hep-ph]].
- [25] V. A. Novikov, L. B. Okun, A. N. Rozanov and M. I. Vysotsky, JETP Lett. **76**, 127 (2002) [Pisma Zh. Eksp. Teor. Fiz. **76**, 158 (2002)] [arXiv:hep-ph/0203132]; Phys. Lett. B **529**, 111 (2002) [arXiv:hep-ph/0111028].
- [26] M. Baak, M. Goebel, J. Haller, A. Hoecker, D. Ludwig, K. Moenig, M. Schott and J. Stelzer, Eur. Phys. J. C **72**, 2003 (2012) [arXiv:1107.0975 [hep-ph]].
- [27] B. Kayser, Phys. Rev. D **24**, 110 (1981).
- [28] C. Giunti, C. W. Kim, J. A. Lee and U. W. Lee, Phys. Rev. D **48**, 4310 (1993) [arXiv:hep-ph/9305276].
- [29] M. Beuthe, Phys. Rept. **375**, 105 (2003) [arXiv:hep-ph/0109119].
- [30] F. J. Botella and L. Chau, Phys. Lett. B **168**, 97 (1986).
- [31] H. Fritzsch and J. Plankl, Phys. Rev. D **35**, 1732 (1987).
- [32] K. Abe *et al.* [T2K Collaboration], Phys. Rev. Lett. **107**, 041801 (2011). [arXiv:1106.2822 [hep-ex]].
- [33] Y. Abe *et al.* [Double Chooz Collaboration], arXiv:1301.2948 [hep-ex].
- [34] F. P. An *et al.* [Daya Bay Collaboration], Chin. Phys. C **37**, 011001 (2013) [arXiv:1210.6327 [hep-ex]].
- [35] D. Meloni, T. Ohlsson and H. Zhang, JHEP **0904**, 033 (2009) [arXiv:0901.1784 [hep-ph]].
- [36] S. Antusch, C. Biggio, E. Fernandez-Martinez, M. B. Gavela and J. Lopez-Pavon, JHEP **0610**, 084 (2006) [arXiv:hep-ph/0607020].
- [37] S. Antusch, J. P. Baumann and E. Fernandez-Martinez, Nucl. Phys. B **810**, 369 (2009) [arXiv:0807.1003 [hep-ph]].
- [38] M. Czakon, J. Gluza and M. Zralek, Acta Phys. Polon. B **32**, 3735 (2001) [arXiv:hep-ph/0109245].
- [39] L. Wolfenstein, Phys. Rev. D **17**, 2369 (1978).
- [40] V. D. Barger, K. Whisnant, S. Pakvasa and R. J. N. Phillips, Phys. Rev. D **22**, 2718 (1980).
- [41] S. P. Mikheev and A. Y. Smirnov, Sov. Phys. JETP **64**, 4 (1986) [Zh. Eksp. Teor. Fiz. **91**, 7 (1986)] [arXiv:0706.0454 [hep-ph]].
- [42] F. J. Botella, C. S. Lim and W. J. Marciano, Phys. Rev. D **35**, 896 (1987).
- [43] M. Galliard and B. Lee, Phys. Rev. D **10**, 897 (1974).